JVI Journals.ASM.org

Straightforward Selection of Broadly Neutralizing Single-Domain Antibodies Targeting the Conserved CD4 and Coreceptor Binding Sites of HIV-1 gp120

Julie Matz,[a,b,c,d] Pascal Kessler,[e] Jérôme Bouchet,[f,g] Olivier Combes,[e] Oscar Henrique Pereira Ramos,[e] Francis Barin,[h] Daniel Baty,[a,b,c,d] Loïc Martin,[e] Serge Benichou,[f,g] Patrick Chames[a,b,c,d]

Inserm,U1068, CRCM, Marseille, France[a]; Institut Paoli-Calmettes, Marseille, France[b]; Aix-Marseille University, Marseille, France[c]; CNRS, UMR7258, CRCM, Marseille, France[d]; CEA, iBiTecS, SIMOPRO, Gif-sur-Yvette, France[e]; Institut Cochin, CNRS UMR8104, Université Paris Descartes, Paris, France[f]; Inserm U1016, Paris, France[g]; Université François Rabelais, Inserm UMR 966, Tours, France[h]

Few broadly neutralizing antibodies targeting determinants of the HIV-1 surface envelope glycoprotein (gp120) involved in sequential binding to host CD4 and chemokine receptors have been characterized. While these epitopes show low diversity among various isolates, HIV-1 employs many strategies to evade humoral immune response toward these sensitive sites, including a carbohydrate shield, low accessibility to these buried cavities, and conformational masking. Using trimeric gp140, free or bound to a CD4 mimic, as immunogens in llamas, we selected a panel of broadly neutralizing single-domain antibodies (sdAbs) that bind to either the CD4 or the coreceptor binding site (CD4BS and CoRBS, respectively). When analyzed as monomers or as homo- or heteromultimers, the best sdAb candidates could not only neutralize viruses carrying subtype B envelopes, corresponding to the Env molecule used for immunization and selection, but were also efficient in neutralizing a broad panel of envelopes from subtypes A, C, G, CRF01_AE, and CRF02_AG, including tier 3 viruses. Interestingly, sdAb multimers exhibited a broader neutralizing activity spectrum than the parental sdAb monomers. The extreme stability and high recombinant production yield combined with their broad neutralization capacity make these sdAbs new potential microbicide candidates for HIV-1 transmission prevention.

Neutralizing antibodies (NAbs) are a natural defense mechanism against virus infections and are the basis of efficient vaccines (1, 2). In the case of HIV-1, NAbs target the viral envelope, a trimeric complex constituted by the noncovalent association of surface gp120 and transmembrane gp41 glycoproteins (3). This complex is responsible for interacting with the primary receptor, CD4, and then with a chemokine coreceptor, CCR5 or CXCR4, expressed at the surface of HIV-1 target cells (4). The surface gp120 glycoprotein elicits both neutralizing and nonneutralizing antibodies during natural infection. Antibodies that lack neutralizing activity are often directed against the gp120 regions that are occluded on the trimer but exposed upon shedding. In contrast, anti-HIV-1 NAbs bind to the functional envelope glycoprotein complex and typically recognize conserved or variable epitopes near the receptor-binding regions.

HIV-1 has evolved many strategies to evade the host humoral immune response, including high sequence variability, protection of sensitive epitopes by a shield of carbohydrate moieties, and conformational and entropic masking (5, 6). Consequently, the neutralizing antibody response during HIV-1 infection is weak and narrow, and only a few monoclonal antibodies with broad neutralization breadth, including among others b12, VRC01, PG16, X5, and 17b, have been isolated (6, 7). The binding mode of b12 and VRC01 has been carefully analyzed, and they were shown to bind to the CD4-binding site (CD4BS) of gp120, mainly using their heavy chain variable region (VH) domain to reach the cavity of gp120 involved in recognition of CD4 (8, 9). Other neutralizing antibodies, such as X5 or 17b, bind gp120 epitopes unveiled by the conformational change induced by CD4 binding and involved in interaction with the coreceptor (10, 11). While these coreceptor binding site (CoRBS) epitopes are buried until the conformational change happens, they become accessible to such antibodies (CD4-induced [CD4i] antibodies) after CD4 binding to gp120. However, Labrijn et al. have shown that conventional Ig antibodies face steric constraints on access to these epitopes due to the close proximity of the viral and cellular membranes, which leaves a very narrow space (10). They have also shown that small antibody fragments derived from CD4i antibodies, such as the 25-kDa single-chain variable fragment (scFv), can reach their epitope and block the infection event more efficiently than the corresponding full-length parental antibody and better even than the corresponding Fab fragment.

Single-domain antibody fragments (sdAbs), derived from camelid antibodies naturally devoid of light chains, are small fragments of 13 kDa, i.e., 1/12 the size of conventional antibodies and half the size of scFv. Because their antigen binding site is constituted by a single VH domain, they usually bind to cavities at the surface of their antigen, often inserting a protruding CDR3 hypervariable loop within the cavity (12). Nonetheless, these fragments not only bind their antigens with low nanomolar affinities but are extremely stable, are very efficiently produced in *Escherichia coli*,

Received 23 February 2012 Accepted 25 October 2012

Published ahead of print 14 November 2012

Address correspondence to Patrick Chames, patrick.chames@inserm.fr, or Serge Benichou, serge.benichou@inserm.fr.

Supplemental material for this article may be found at http://dx.doi.org/10.1128/JVI.00461-12.

doi:10.1128/JVI.00461-12

and present a large degree of homology with the VH3 subset of human VH genes. Thus, because of their small size and their tendency to bind cavities, they have been proposed as good neutralizing antibody candidates. If CD4BS sdAbs with good neutralizing capacities have already been isolated (13, 14), to our knowledge, no CoRBS sdAb has yet been discovered to date.

Using the scorpion toxin scyllatoxin as a small disulfide-stabilized structural scaffold, we have developed a series of small CD4 mimics that present optimal interaction with gp120 and bind to viral particles and diverse HIV-1 envelopes with CD4-like affinity. Interestingly, they possess CD4 functional properties, including the ability to unmask gp120 conserved neutralization epitopes that are cryptic on the unbound glycoprotein (15–19). In the present work, to increase the chance of selecting neutralizing sdAbs targeting the CD4 and coreceptor binding sites of gp120, we have immunized llamas with gp140 (trimeric version of gp120 bound to the gp41 ectodomain), either free or cross-linked to a CD4 mimic (16). The last version was aimed to enhance CD4i epitope exposure. Various selection strategies have led to the isolation of several CD4BS and CoRBS single-domain antibodies with broad neutralization properties.

MATERIALS AND METHODS

Preparation of recombinant Env constructs and CD4 mimics. For simplicity, gp120 and gp140 stemming from the SF162 strain are referred to as gp120 and gp140. Glycoproteins from other strains are explicitly identified (for instance, gp120YU2).

The Freestyle 293 expression system (Life Technologies, Invitrogen) was used to generate transient cells expressing the various gp120, gp120YU2, and gp120CN54 monomers or the gp140 and gp140YU2 trimeric form, using Freemax as the transfection reagent. The various envelopes were purified as previously described by miniCD4 affinity chromatography (17). They were then used as such or cross-linked to miniCD4 derivative M64U1-SH through disulfide bond formation as described previously (16). Wild-type gp140YU2, gp140YU2 D368R (having a change from Asp to Arg at position 368), gp140YU2 I420R, and the gp140YU2 I423M N425K G431E triple mutant were kindly provided by Richard Wyatt (Department of Immunology and Microbial Science, The Scripps Research Institute, La Jolla, CA).

The miniCD4 derivatives M48U1 and M64U1-SH were synthesized and purified by reverse-phase chromatography as described earlier (16) and characterized by mass spectrometry.

For the fluorescence polarization assay, we obtained in the same way a specific miniCD4, M64-Fluo, which was coupled to fluorescein at the εNH_2 of Lys11 through a short polyethylene glycol (PEG) linker obtained from 8-amino-3,6-dioxaoctanoic acid.

The M64 sequence is TpaNLKWCQKRCKSLGLLGRCAdPTFCACV-NH_2, where Tpa stands for 3-mercaptopropanoyl (-COCH2CH2SH, equivalent to an amineless cysteinyl residue) and dP for D-proline.

Immunization and library construction. Two llamas (*Lama glama*) were immunized with either free gp140 or purified cross-linked gp140-S-S-M64U1 complex. Each llama received 4 injections of 250 μg of antigen with Freund's incomplete adjuvant at 3-week intervals. Two weeks after the last immunization, 400 ml of blood was collected per llama. Total RNA was isolated from peripheral blood lymphocytes. IgG RNA sequences were reverse transcribed with reverse transcriptase using primer 3′CH2-2 (GGTACGTGCTGTTGAACTGTTCC). VH and V_HH (variable domains of camelid heavy-chain antibodies) genes of IgG were amplified by PCR using primer 3′CH2-2 and a mix of 5′VH1/3/4-Sfi (20). After gel purification of fragments corresponding to V_HH genes, amplifications were carried out by PCR using primers 3′VHH-Not (described in reference 20) and a mix of 5′VH1/3/4 Sfi. These genes were subcloned using SfiI and NotI restriction sites.

Selection and screening by phage display. Libraries were rescued using KM13 helper phage to carry out selections by phage display.

First, basic selections were performed with free gp120 or gp120-S-S-M64U1 immobilized on Epoxy Dynabeads via monoclonal antibody (MAb) D7324 (Aalto Bio Reagents, Dublin, Ireland), and all phage-sdAbs were eluted by trypsin treatment (1 h at room temperature, trypsin at 1 mg/ml). In some cases, a competitive elution was performed using miniCD4 M48U1 (21), followed by a trypsin treatment. Selections were also performed using the trimeric gp140 or gp140-S-S-M64U1 bound directly to Epoxy Dynabeads and using trypsin elution.

Two last selections were designed to obtain broad-spectrum sdAbs. The first rounds were done using free gp120YU2 or gp120-S-S-M64U1, and the second rounds were performed using free gp120CN54 and gp120YU2-S-S-M64U1, respectively, with trypsin elution.

Selected clones were sequenced to identify distinct sdAbs.

Construction of multivalent proteins. Genes for homotrivalent constructs of two sdAbs of interest, JM2 and JM4, with $(G_4S)_7$ linkers (denoted as "x" in construct names) between each domain were obtained from Geneart and subcloned into phagemid pHEN. To obtain the coding sequence of two-domain versions (JM2x2, JM2x3, JM2x4, JM2x5, JM4x2, JM4x3, JM4x4, and JM4x5), genes of sdAbs JM2, JM3, JM4, and JM5 were amplified by PCR using primers Trim2For (AGTGGTGGCGGAGGTAGCGCTAGCGAGG TGCAGCTGGTGGAG) and Trim3Rev (TGAGATGAGTTTTTGTTCT GCGGCCGCTGAGGAGACGGTGACCTG). PCR products were cloned into the digested trivalent plasmid by using the InFusion system (Clontech). To create the remaining bivalent-protein genes (JM3x2, JM3x3, JM3x4, JM3x5, JM5x2, JM5x3, JM5x4, and JM5x5), PCR amplifications were performed using primers Trim1For (CTCGCGGCCCAGCCGGCC ATGGCCGAGGTGCAGCTG) and Trim1Rev (CCGCTGCCACCTCCC CCCAGGCCTGAGGAGACAGTGACCTG) to amplify the JM3 and JM5 genes, which were substituted for the first sdAb gene of previous constructs using the InFusion system (the cloning scheme is illustrated in Fig. S1 in the supplemental material) (22). All constructs were checked by sequencing.

Production and purification of sdAbs and multivalent proteins. All sdAbs were produced in *E. coli* BL21(DE3). Production was done by seeding 400 ml of 2TY-Amp-50x5052 (autoinductive medium) (23). The culture was incubated first for 3 h at 37°C and then overnight at 30°C. All multivalent proteins were produced in *E. coli* BL21(DE3) by seeding 400 ml of 2TY-Amp, and production was induced by the addition of 0.1 mM isopropyl-β-D-thiogalactopyranoside (IPTG) when the optical density at 600 nm (OD_{600}) reached 0.4 to 0.7.

For purification, bacteria were lysed using BugBuster protein extraction reagent (Novagen) containing lysozyme and Benzonase. Supernatants were applied to Talon beads (Clontech), and elution of 6His-sdAbs and multivalent proteins was done by the addition of imidazole. Lastly, elution buffer was changed for phosphate-buffered saline (PBS) using Vivaspin with a 5-kDa molecular-mass cutoff (GE HealthCare Life Science). sdAbs were stocked in PBS at −20°C. Most sdAbs could be produced with yields in the range of 10 to 100 mg/liter culture, while yields were about 1 mg/liter culture for multivalent proteins. Multivalent constructs that were not easily expressed were not studied further.

Characterization of binding to different subtypes of gp120 and gp140. All steps to characterize binding to the different subtypes of gp120 and gp140 were performed at room temperature with mixing, except for bead or plate coating. Washes were carried out between each step.

For enzyme-linked immunosorbent assay (ELISA) of gp120, Epoxy beads were coated (Dynabead, Invitrogen) with MAb D7324, with 8×10^5 beads per well being coated with 0.2 μg of MAb D7324 per well. Coating was carried out for 48 h at 4°C on a wheel. Beads were blocked for 1 h with 2% milk-PBS (MPBS). gp120 was added at 10 nM for 2 h, and beads were dispensed into a preblocked 96-well plate. sdAbs were added at 10 μg/ml for 1 h. Bound sdAbs were detected using horseradish peroxidase (HRP)-coupled anti-c-myc antibody (clone 9E10) that was incubated for 1 h, and staining was performed using ABTS [2,2′-azinobis(3-ethylbenzthiazo-

linesulfonic acid)]-based solution. The optical density was followed at 450 nm.

For ELISA of gp140, the same protocol was used, with 0.1 μg of gp140 being used to directly coat 8×10^5 Epoxy beads per well for 48 h at 4°C on a wheel. gp120 and gp140 were used free or covalently cross-linked to M64U1-SH.

Cells. TZM-bl reporter cells (HeLa $CD4^+$ $CXCR4^+$ $CCR5^+$ carrying the luciferase gene under the control of the HIV-1 long terminal repeat [LTR]) (24) and human embryonic kidney 293T cells were grown in DMEM (Dulbecco's modified Eagle's medium) supplemented with 10% fetal calf serum (FCS) and antibiotic/antifungal at 37°C under 5% CO2.

Single-round pseudovirion production and neutralization assay. 293T cells were seeded in T75 flasks at a density of 3×10^6 cells/flask and transfected 24 h later by the calcium phosphate precipitation method with a DNA mix containing the HIV-1 packaging plasmid (pCMVΔR8.2) (25), the HIV-1 transducing vector containing the *tat* gene (pHIvec2-GFP) (26), and a plasmid encoding the HIV-1 envelope glycoprotein (or vesicular stomatitis virus G glycoprotein [VSV-G] as control) at concentrations of 8, 8, and 2 μg/T75 flask, respectively. Medium was removed 6 h after transfection, and 10 ml of complete medium was added. Seventy-two hours after transfection, supernatants containing pseudovirions were collected, spun to remove cell debris, filtered through 0.45-μm-pore-size filters, and stored at −80°C until use in neutralization experiments. Levels of virus production were measured by HIV-1 Cap24 quantification in ELISA (Innogenetics). To determine the $TCID_{50}$ (50% tissue culture infective dose), 5-fold dilutions were carried out in 96-well plates with once-frozen cryovial of each pseudovirion production. Then, 10^4 TZM-bl cells/well were added and plates were incubated at 37°C for 48 h. After cell lysis using luciferase cell culture lysis reagent (Promega), luciferase activity was measured using a luciferase assay kit (Promega).

Plasmids encoding HIV-1 envelope glycoproteins (pSVIII-93BR029.2, -92UG975.0, -93BR019.4, -92BR025.9, -91US005.11, -92RW020.5, -92UG037.8, -92HT593.1, -93MW965.26, -92UG024.2, -92UG021.16, -93TH966.8, and -93TH976.17) were obtained from the NIH AIDS Research and Reference Reagent Program. pSVIIIENV HxBC2, pEnv 89.6, pEnv YU2, and pEnv VSV-G plasmids have been described previously (27).

For the neutralization assay, pseudovirions (100 $TCID_{50}$) were preincubated in 96-well plates with monovalent or multivalent sdAbs at 10 μM and 5 μM, respectively. Plates were incubated for 1 h at 37°C. Then, 10^4 TZM-bl cells/well were added and plates were incubated at 37°C for 48 h. Luciferase activity was measured as described above. The 50% inhibitory concentrations (IC_{50}s) were determined for sdAbs able to inhibit virus entry into TZM-bl cells. In the same manner, virions (100 $TCID_{50}$) were preincubated in 96-well plates with different concentrations of sdAbs. Plates were incubated for 1 h at 37°C. Then, 10^4 cells/well were added and plates were incubated at 37°C for 48 h. Luciferase activity was measured as described above. IC_{50}s were calculated using Prism software (GraphPad Software, Inc., San Diego, CA).

Neutralization assay on resistant primary isolates. The virus panel included two T-cell-line-adapted (TCLA) strains highly sensitive to neutralization (tier 1A; NL4.3 and MN) and nine primary isolates selected for their high (tier 1B), moderate (tier 2), or low (tier 3) sensitivity to neutralization. Four primary isolates (BX08, BIG, FRO, and KON) of two different clades (B and CRF02_AG) were reported in previous studies (28–30). We added five primary isolates, including four viruses (94UG103, 92BR020, 93IN905, and 92TH021, of clades A, B, C, and CRF01_AE, respectively) identified as indicators for cross-clade neutralization (31) and one moderately resistant virus (92RW020, clade A) (31). This virus panel included viruses that were resistant to almost all the broadly neutralizing human monoclonal antibodies that we tested (2G12, b12, 2F5, 4E10, PG9, and PG16). Monoclonal antibodies b12, 2G12, 4E10, and 2F5 were provided by Polymun Scientific (Vienna, Austria). PG9 and PG16 were kindly provided by P. Poignard (The Scripps Research Institute, La Jolla, CA) through the Neutralizing Antibody Consortium of the International AIDS Vaccine Initiative (IAVI, New York, NY). The virus stocks for the neutralization assays were prepared by passaging the strains only once or twice on phytohemagglutinin-stimulated peripheral blood mononuclear cells (PBMCs) from HIV-negative healthy blood donors. The same stock of each isolate was used for the entire study. Infectious titers were determined by infection of 1×10^4 TZM-bl cells with 100 μl of serial 5-fold dilutions of the viral stocks in quadruplicate in the presence of 30 μg/ml of DEAE-dextran. Infection levels were determined after 48 h, using the Bright Glo luciferase assay (Promega) and a Centro LB 960 luminometer (Berthold Technologies) to measure luciferase activity in cell lysates. Results with relative light unit (RLU) values of >2.5 times that of the negative control (cells alone) were considered positive.

Aliquots of 50 μl of the dilution corresponding to 100 $TCID_{50}$ of each virus stock were incubated for 1 h at 37°C with 11 μl of 3-fold serial dilutions of each antibody, starting at 50 μg/ml for all the reagents except PG9 and PG16, for which the starting dilution was 10 μg/ml. The virus-serum mixture was then used to infect 10,000 TZM-bl cells in a 96-well microplate in the presence of 30 μg/ml DEAE-dextran. Infection levels were determined after 48 h through determination of the luciferase activity in cell lysates, as described above. IC_{50}s are expressed as the mean amounts required to decrease the relative light units (RLU) by 50%. The results are expressed as the mean values of the assays performed in duplicate.

Competition between sdAbs using sdAb and phage-sdAb formats. All steps except the coating were performed at room temperature with mixing. Washes were carried out between each step except before the addition of phage-sdAbs.

Epoxy beads were coated with MAb D7324 as described above. Beads were blocked for 1 h with 2% MPBS. Free gp120 or gp120-S-S-M64U1 was incubated at 10 nM for 2 h at room temperature. Serial dilutions from 10 μM to 0.01 nM sdAbs were added. After 1 h, subsaturating concentrations of phage-sdAbs were added. After 1 h of incubation followed by washes, HRP-coupled M13 antibody was added for 1 h and staining was done using ABTS-based solution. The OD_{450} was measured.

Characterization of sdAbs by surface plasmon resonance (SPR). Experiments were conducted at 25°C with a 30 μl/min flow rate in HBS (HEPES-buffered saline, 3 mM EDTA, 0.05% Biacore surfactant, pH 7.4) with a Biacore 3000 instrument (Biacore AB, Uppsala, Sweden). sdAbs were immobilized at a level of 1,000 to 2,000 response units (RU) by using the amine coupling kit [*N*-hydroxysuccinimide–1-ethyl-3-(3-dimethylaminopropyl) carbodiimide (NHS-EDC)] provided by the manufacturer. gp120 and gp140 of different subtypes were tested complexed or not with miniCD4 (notably M48U1) or soluble CD4 (sCD4) to determine the sdAb specificities. CD4i antibodies X5 and 17b and CD4BS antibody b12 were used in competition assays using ranges of dilution from 250 nM to 0.37 nM. Calculations were done using the BiaEval 3.2 software furnished with the Biacore instrument.

Characterization of sdAbs JM2, JM3, JM4, JM5, and JM7 by fluorescence polarization. Competitive fluorescence polarization was assessed as previously described by Stricher et al. (32), using M64-Fluo instead of fluorescein-CD4M33. Briefly, competition assays were performed in triplicate by mixing 7 μl of serial sdAb dilutions (or M48U1), 7 μl of M64-Fluo (2 nM final concentration), and 7 μl of gp120 (8 nM final concentration). The fluorescence polarization was determined after 40 min of equilibration time. Results were expressed as percentages of the results of control experiments, in the absence of competitor.

Cell surface CCR5 chemokine receptor binding assays. The effects of sdAbs binding to gp120 on the interaction of the latter with its cellular coreceptor CCR5 were investigated by flow cytometry (FACSCalibur; BD Biosciences) using adherent CHO-K1 cells overexpressing CCR5 (33). Briefly, 1 μM gp120 was preincubated or not with 3 molar equivalents (eq) of sCD4 (Progenic, Tarrytown, NY) or 5 eq miniCD4 M48U1 for 1 h at room temperature. The mixtures were then diluted to 2 nM gp120 with PBS-bovine serum albumin (BSA) 0.5%, pH 7.4. For competition purposes, 100 nM each given sdAb was added. One hundred microliters of

this solution was mixed with 2×10^5 $CCR5^+$ cells. After 2 h of incubation at 4°C, cells were washed with PBS-BSA 0.5% and incubated with MAb D7324 (1:1,000). A phycoerythrin-tagged antibody (1:500) directed against MAb D7324 further detected envelope glycoprotein binding to CCR5 coreceptor.

Epitope mapping by competitive ELISA using mutant Env proteins. Shortly, Maxisorp 96-well plates were coated with sdAbs (500 ng/well, 2 h at room temperature). Next, wells were saturated with PBS containing 3% BSA (overnight, 4°C) and washed (25 mM Tris-HCl, 50 mM NaCl, Tween 0.1%, pH 7.4), and serial dilutions of wild-type gp140YU2 trimer or the D368R, I420R, or I423M N425K G431E triple mutant (34) were added in the absence (for JM2-coated wells) or presence (for JM3-, JM4-, JM5-, and JM7-coated wells) of miniCD4 M48U1 at 10 molar eq. After 2 h of incubation at room temperature, wells were washed, and bound gp140 proteins were detected by sequential recognition using D7324 antibody (1:1,000) and donkey anti-sheep IgG HRP-coupled antibody (1:5,000) (Jackson ImmunoResearch). Plates were read at 450 nm 20 min after the addition of 3,3′,5,5′-tetramethylbenzidine (TMB).

Determination of affinity by SPR. Experiments were conducted as described above but using an R_{max} of 200 RU for the sdAb immobilization. Dilutions of Env (from 200 nM to 0.4 nM) were tested to determine the affinity of sdAbs JM2, JM4, and JM7. Calculations were performed using the BiaEval 3.2 software.

RESULTS

Selection of anti-Env sdAbs. To increase the chance of isolating single-domain antibodies (sdAbs) targeting various envelope epitopes, two llamas were immunized with four injections of either the trimeric gp140 (SF162 HIV-1 strain) or the same trimeric form covalently cross-linked to a CD4 mimic (gp140-S-S-M64U1) to favor the selection of CD4i sdAb binders. The V_HH genes from immunized animals were then amplified from PBMCs and were cloned into a phagemid vector. Electroporation yielded around 10^8 independent clones for each library. Various selection strategies were then performed to increase the chance of isolating sdAbs against a large number of relevant epitopes. Antigens were immobilized via the interaction with MAb D7324, targeting the C-terminal end of gp120, and basic strategies included selections on gp120 monomer, either free or cross-linked to a CD4 mimic to unveil CD4i epitopes. A similar approach was performed using the trimeric free gp140 and the cross-linked complex gp140-S-S-M64U1. After two rounds of selection, positive clones were identified by phage ELISA using the antigen used for selection in a primary screening. Positive clones were sequenced (Fig. 1), and representative clones of each family were produced and purified as soluble sdAbs to be further characterized by a secondary screening using a panel of antigens.

The results of binding analysis of the selected sdAbs to different Env and Env-S-S-M64U1 antigens are reported in Fig. 2. Based on their capacity to bind to various conformations of gp120 and gp140, four types of anti-Env sdAbs could be defined. (i) Clones JM1 and JM2 behaved as CD4BS binders, as they could bind to free gp120 and gp140 but not to the same envelopes cross-linked to the CD4 mimic (Fig. 2A). JM2 yielded a higher response and was therefore selected for further analysis. (ii) Clones JM3, JM4, and JM5 bound to free or miniCD4-cross-linked gp120 and gp140 (Fig. 2B), suggesting that they do not share their epitope with JM2. In this assay, JM5 displayed a tendency toward a better affinity for cross-linked Env, suggesting a CD4i behavior. (iii) Clone JM7 behaved more drastically, since it could only bind to cross-linked gp120- or gp140-S-S-M64U1 complexes. (iv) Finally, clones JM8 and JM9 yielded no signal against any gp120 form but yielded high

	Frequency	CDR1	CDR2	CDR3
JM1	**6**	**GSISSFNA**	**RIKNGGGS**	**VVQRRNDYTIFTTY**
JM2	7	--------	--------	--------I-----
JM3	**23**	**GFTLEDYS**	**CISDSDGRT**	**ATDCTVVPSLLYAMDS**
JM4	13	----DY--	C--------	---C--D-----V--Y
JM5	10	--S-DY-A	C--S-E-S-	---C--T-GT-----N
JM6	**2**	**GITLDYYD**	**CISSSDGST**	**ATVSLVGTI.....YCEDEYDY**
JM13	2	-F------	C------T-	-S----------C------
JM7	8	RF--P---	C--------	---TI-AG----------TC------
JM10	3	-F------	C--------	----M--SW----------C-E----
JM12	4	-F-----T	C-N----T-	--SD-GTYGTTWFSPEAILSPY----
JM8	**2**	**GSIRSINN**	**AMTTSGIT**	**RVGSWYQPHDY**
JM9	5	---VG--A	VI-S--S-	KM-----SD--
JM11	**1**	**GLTFSNYA**	**AITWSGGSA**	**AADRDVTILTVTNLALYDY**
JM17	**1**	**GSIFSIYA**	**AITSSGST**	**NADGLGWGNY**
JM18	**1**	**GRTFSPYA**	**AISWNGGNT**	**AASSKYRVVLDVNEYDW**

FIG 1 Sequences of anti-Env sdAbs. Selected clones were sequenced and aligned following the IMGT (international ImMunoGeneTics information system) numbering. Four families were created in accordance with homology in the complementarity-determining region (CDR). Three unique clone families were selected. The total number of times each clone was retrieved is indicated as frequency.

signals on free and cross-linked trimeric gp140 (Fig. 2C). Interestingly, these two last clones were only retrieved during selections performed on trimeric gp140. They were thus considered gp140 specific. None of the sdAbs were found positive on miniCD4 by ELISA (data not shown).

Neutralizing activity of anti-Env sdAbs. A single-round infection assay was first set up to determine the capability of these monovalent sdAbs to block HIV-1 infection of a panel of pseudotyped virions carrying various envelope glycoproteins from subtypes A, B, C, G, or CRF01_AE. sdAbs were compared to the well-described broadly neutralizing antibody b12. Virus particles pseudotyped with VSV-G were used as a specificity control in this neutralization assay. Interestingly, a first screening performed using 10 μM each sdAb revealed some neutralization properties for most selected sdAbs, except JM7 (Fig. 3). As expected, sdAbs were able to efficiently neutralize pseudovirions carrying X4- and R5-tropic envelopes of subtype B, since immunizations and selections were performed with subtype B or subtype B′/C envelopes. More interestingly, sdAbs JM3, JM4, and to a lesser extent JM5 could neutralize most tested pseudovirions, including those pseudotyped with subtypes A, C, G, and CRF01_AE envelopes. Determination of the IC_{50}s, which ranged between 0.2 and 40 μg/ml, confirmed these observations (Table 1). In comparison, the IC_{50}s measured for the b12 monoclonal antibody ranged between 0.005 and 1.5 μg/ml, but its neutralizing activity was restricted to subtype B envelopes at these concentrations.

To further define the neutralization ability of these sdAbs, assays using primary viruses were performed. This virus panel included two T-cell-line-adapted (TCLA) strains highly sensitive to neutralization (tier 1A; NL4.3 and MN) and nine primary isolates selected for their high (tier 1B), moderate (tier 2), or low (tier 3) sensitivity to neutralization. As shown in Table 2, JM2 and JM5 were able to neutralize 1 and 2 of these 11 viruses, respectively, and

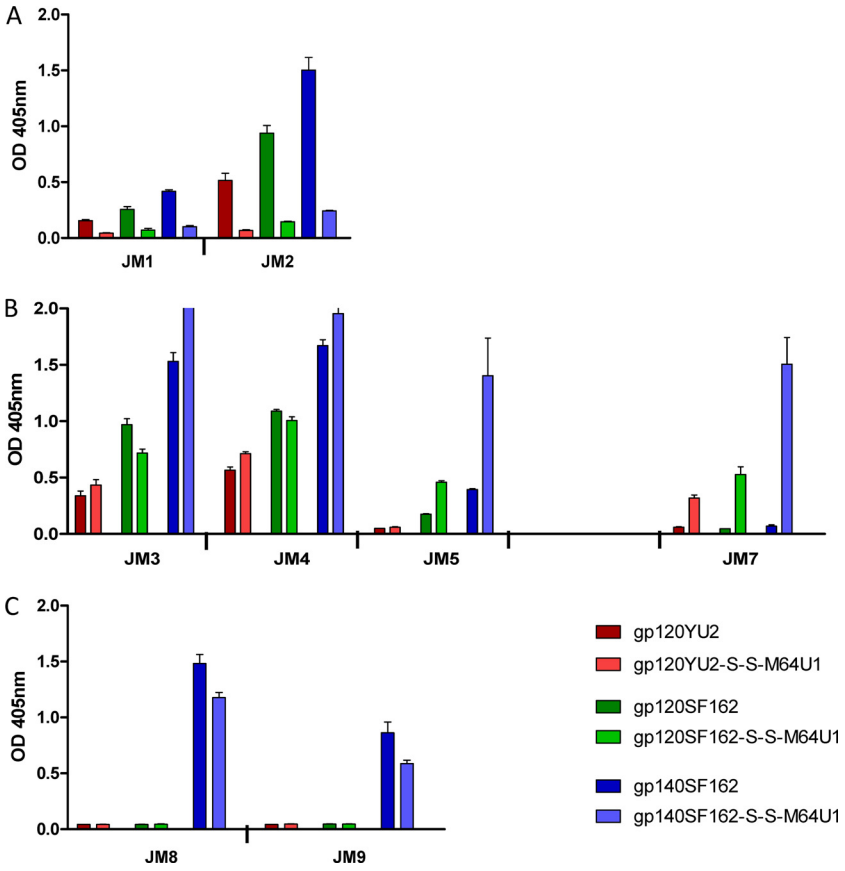

FIG 2 sdAb binding on different conformations and strains of HIV-1 Env, followed by ELISA. sdAbs binding to gp120 (bound via the D7324 antibody to Epoxy beads) or to gp140 (directly immobilized on Epoxy beads) were detected via a peroxidase-labeled anti-c-myc Ab. Histograms correspond to the three main families of sdAbs selected. (A) JM1 and JM2 clones bind preferentially to the free form of Env. (B) JM3, JM4, and JM5 bind both Env forms, while JM7 only binds to the cross-linked Env. (C) JM8 and JM9 bind exclusively to the gp140 trimeric form of Env. Shown are the results of one experiment representative of at least three. Error bars represent standard deviations of the means.

JM3 neutralized 5 of them, outperforming well-known broadly neutralizing antibodies such as 2G12, b12, 2F5, 4E10, and PG9. JM4 could neutralize 7 of these 11 viruses, thereby matching or outperforming all broadly neutralizing antibodies tested in this assay in terms of neutralization breadth. The fact that the sdAbs, except JM3, were not efficient at neutralizing the sensitive MN strain might suggest a specific mode of interaction with or a particular accessibility to the targeted epitopes.

Characterization of the anti-Env sdAb epitopes. Several experimental approaches were designed to better characterize the epitopes targeted by these anti-Env sdAbs. We first determined whether some of these Env binders recognized overlapping epitopes by using competitive ELISA between purified sdAbs and phage-sdAbs for binding to gp140 (Fig. 4A) or gp140-S-S-M64U1 (Fig. 4B). As expected, all sdAbs competed with themselves.

In the absence of competitor, phage-sdAb JM2 (phage-JM2) yielded a nearly saturating signal on free Env but could still bind to the miniCD4-cross-linked Env, albeit at a reduced level. This is surprising since the purified sdAb JM2 only led to a very faint signal on the same antigen (Fig. 2). This result could be explained by the presence of a small percentage of free Env in the complexed form in conjunction with the very high sensitivity of the phage ELISA format (each phage particle being detected by several dozens of anti-M13 HRP-labeled antibodies bound to the phage capsid). In the presence of competitors on free Env, phage-JM2 binding was clearly hampered by the presence of MAb b12 but not by MAb X5 (Fig. 4A), corroborating the CD4BS nature of this sdAb. Of note, the residual binding of phage-JM2 on miniCD4-cross-linked Env was also efficiently competed by b12, confirming the hypothesis regarding the presence of residual free Env in this preparation.

In the absence of competitor, phage-JM3, -JM4, and -JM5 yielded higher signals on miniCD4-cross-linked Env than on free Env (Fig. 4B versus A), suggesting a CD4i behavior. Moreover, binding of phage-JM7 happened only on the cross-linked form (Fig. 4B). As expected, JM3, JM4, and JM5 behaved similarly and competed each other on both miniCD4-cross-linked and free Env, indicating that they bind to overlapping epitopes. JM7 could also compete with phage-JM3, -JM4, and -JM5 but only on the cross-linked form, as expected since it cannot bind free Env. Phage-JM8 bound to both forms of Env and did not compete with other sdAbs.

More surprisingly, phage-JM2 binding to free Env was affected by the presence of sdAbs JM3 and JM4 but not by CD4i MAb X5 (35). Similarly, binding of phage-JM3, -JM4, and -JM5 to free Env was also hampered by JM2 or the CD4BS MAb b12 (Fig. 4A). The influence of sdAb JM2 was not observed on cross-linked Env (Fig. 4B), logically, since this sdAb can hardly bind to this form (Fig. 2).

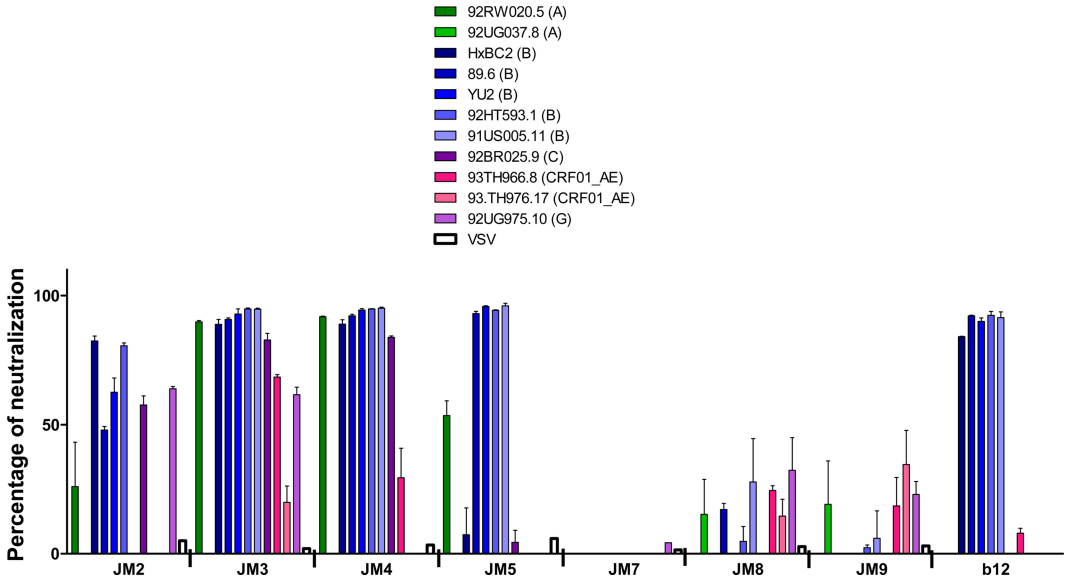

FIG 3 sdAb neutralization ability toward different pseudovirion strains. Each sdAb was tested in a single-round neutralization assay as described in Materials and Methods, using TZM-bl cells as target cells. Pseudovirions (100 $TCID_{50}$) carrying various envelope glycoproteins from different HIV-1 subtypes were preincubated with purified sdAbs at 10 μM in 96-well plates for 1 h at 37°C. TZM-bl cells were then added, and luciferase activity was measured 48 h later. Values are expressed as percentage of neutralization relative to the luciferase activity measured in the absence of sdAb. Shown are the results of one experiment representative of at least three. Error bars represent standard deviations of the means.

These results suggest that JM2 binding may stabilize an Env conformation that prevents recognition by phage-JM3, -JM4, and -JM5, and vice versa. Alternatively, the orientation of the various antibodies and large phage-V_HH particles with respect to gp140 may engender steric clashes. Together, these data support a common recognition of CD4i epitopes for JM3, JM4, and JM5 and targeting of the Env CD4BS for JM2.

Surface plasmon resonance (SPR) analyses using high-immobilization-density chips were used to confirm ELISA data and to roughly estimate the binding profiles of the neutralizing anti-Env sdAbs against various Env antigens (Fig. 5). As expected for a CD4BS antibody, JM2 could clearly bind to the uncomplexed form of gp120 but not to its complexed form (Fig. 5A). On monomeric gp120 (Fig. 5B), JM3, JM4, and JM5, displaying a CD4i profile by ELISA, yielded higher signals with complexed gp120 than with uncomplexed gp120, and similar results were observed with the trimeric form of Env (gp140) (Fig. 5C), validating a CD4i behavior. Of note, and in contrast to JM4 and JM5 or the well-defined CD4i MAb X5 used as a control (11), JM3 did not bind more efficiently to gp120 complexed to a soluble recombinant CD4 molecule (sCD4) than to free gp120. This observation might be related to steric clashes between JM3 and CD4, which do not happen with the smaller miniCD4. As observed in ELISA (Fig. 2), JM7 was found exclusively positive on the gp120-miniCD4 complex and did not bind at all to free gp120. However, unlike other CD4i sdAbs or MAb X5, JM7 was also found negative on gp120 complexed to sCD4. Since we checked by fluorescence polarization that this sdAb was unable to bind directly to the CD4 mimic constructs (data not shown), this observation suggests that JM7 may recognize an epitope specifically formed by the association of gp120 and the CD4 mimic. Another possible explanation would be that JM7 can only bind gp120 in the CD4-bound state, which is mimicked here by the miniCD4, and that the orientation of JM7 allows the presence of a small miniCD4 (3 kDa) but clashes with the much bigger sCD4 molecule (about 20 kDa). Nevertheless, this observation explains why this sdAb was unable to neutralize

TABLE 1 IC_{50}s of monovalent and multivalent sdAbs on pseudovirions carrying various HIV-1 envelope glycoproteins

Virus[b]	Subtype	IC_{50} in TZM-bl cells (μg/ml)[a]																		
		JM2	JM3	JM4	JM5	JM8	JM9	JM2x2	JM2x4	JM2x5	JM3x3	JM3x5	JM4x2	JM4x3	JM4x5	JM5x2	JM5x3	JM5x5	JM4x4x4	b12
92RW020.5	A	X	4.4	23.3	X	●	●	X	1.5*	0.8	27.5	●	X	●	X	1.6	18.9	●	48*	●
92UG037.8	A	●	●	●	●	X	X	40.8	●	●	46.5	●	●	●	●	47.3	35.2	●	X	●
HxBC2	B	0.2	9.9	0.7	●	●	●	0.2	0.6	3.7	16.1	●	12.9	21.4	54.0	15.1	134.4	●	73.8	0.005
89.6	B	X	0.7	0.5	2.6	X	●	X	●	●	1.6	11.0	●	7.0	0.8	29.5	4.8	19.0	8.3	0.14
YU2	B	30	8.7	6.6	3.2	●	●	28.5	92.8*	X	16.7	85.1*	96*	60.8*	36.4*	10.9	20.3	5.9*	17*	1.53
92HT593.1	B	5	1.4	1.2	1.1	●	●	18.8	49.6*	15.4*	8.0	X	10.3	32*	12.2	19.3	12.4	X	X	1.04
91US005.11	B	●	3.6	4.2	3.8	X	●	57.3	108.9*	●	14.7	●	●	27.4*	32*	32.0	16.3	54.1*	48*	1.14
92BR025.9	C	11.4	8.8	9.7	●	●	●	X	X	X	13.6	●	99.6*	32*	46.2*	36.2	42.2	●	96*	●
93TH966.8	A/E	●	2.3	X	●	X	X	42.6	X	●	27.3	●	●	45.1*	●	●	37.9	●	59	●
93TH976.17	A/E	●	●	●	●	X	X	36.8	●	●	83.8	●	●	●	●	90.9	20.8	●	168.96	●
92UG975.10	G	43.8	80.6*	●	●	X	X	33.3	●	●	57.9	●	●	●	●	75.0	134.4	●	X	●

[a] ●, no neutralization was observed at the highest tested concentration (150 μg/ml); X, IC_{50} could not be calculated but some neutralization was observed; shaded cell, IC_{50} determined as 50% of inhibitor effect; *, complete neutralization was not observed at the highest tested concentration of 150 μg/ml.

[b] 92RW020.5, 92UG037.8, and 92BR025.9 are tier 1; 89.6 and YU2 are tier 2.

TABLE 2 IC_{50}s of monovalent sdAbs on viruses with various levels of sensitivity to neutralization[a]

Virus	Clade	Tier	IC_{50} in TZM-bl cells (μg/ml)[b]									
			JM2	JM3	JM4	JM5	2G12	b12	2F5	4E10	PG9	PG16
94UG103	A	2	>50	12.30	13.40	>50	>50	>50	>50	>50	1.78	<0.12
92RW020	A	2	>50	>50	>50	>50	4.5	>50	>50	>50	0.14	0.87
NL4.3	B	1A	1.45	1.43	0.02	29.60	NT	NT	NT	NT	NT	NT
MN	B	1A	>50	4.66	>50	>50	<0.12	<0.12	<0.12	<0.12	<0.12	<0.12
BX08	B	1B	>50	>50	14.45	>50	NT	NT	NT	NT	NT	NT
BIG	B	2/3	>50	>50	30.00	>50	43.53	2.33	>50	>50	>10	<0.12
FRO	B	2/3	>50	29.60	28.30	44.40	>50	>50	26.36	>50	>10	>10
92BR020	B	2	>50	>50	>50	>50	>50	>50	>50	>50	>10	>10
93IN905	C	2	>50	>50	41.80	>50	>50	>50	>50	>50	3.81	>10
92TH021	CRF01_AE	2	>50	>50	>50	>50	>50	>50	>50	>50	>10	>10
KON	CRF02_AG	2/3	>50	45.23	22.62	>50	>50	>50	>50	>50	<0.12	<0.12

[a] Viruses used were two T-cell-line-adapted strains highly sensitive to neutralization (tier 1A; NL4.3 and MN) and nine primary isolates selected for their high (tier 1B), moderate (tier 2) or low (tier 3) sensitivity to neutralization.

[b] Starting dilutions were 50 μg/ml for all antibodies except PG9 and PG16, for which the starting dilution was 10 μg/ml. NT, not tested. Shading highlights neutralizing effects.

all the tested viruses (Fig. 3), despite behavior quite similar to that of sdAbs JM3, JM4, and JM5 (Fig. 4).

Characterization of the CD4BS sdAb JM2. Since the ELISA and SPR results suggested that JM2 was targeting the gp120 CD4BS, we confirmed this hypothesis by performing fluorescence polarization experiments on gp120, using a fluorescent miniCD4 probe (M64-Fluo) and sdAbs including JM2 or the CD4 mimic M48U1 as competitors. This approach relies on the fact that a small molecule (such as miniCD4) rotates fast in solution and exhibits low fluorescence polarization whereas a large molecule (such as gp120-miniCD4 complex) exhibits a higher fluorescence polarization because of its slower motion under the same conditions. Thus, changes in fluorescence polarization can reflect the association or dissociation between molecules of interest, in our case, M64-Fluo and gp120. As shown in Fig. 6A, JM2, as well as M48U1, efficiently competed with the M64-Fluo probe for gp120 binding, thereby confirming that JM2 is a CD4BS ligand. M48U1 outperformed JM2, as it possesses a subnanomolar affinity for gp120 (21). This experiment was also conducted with JM3, JM4, JM5, and JM7, and no competition was observed.

Since MAb b12 is a well-characterized CD4BS antibody, competition experiments were also performed by SPR using this antibody. As shown in Fig. 6B, MAb b12 competed with sdAb JM2 for binding to unliganded gp120, thus confirming that this sdAb behaves as a CD4BS binder.

Finally, when analyzed by flow cytometry on CCR5-expressing cells, JM2 was also shown to block gp120 binding to CCR5, likely through stabilization of gp120 in a conformation which does not allow CCR5 binding (Fig. 7A). Furthermore, the subsequent addition of sCD4 or M48U1 could not restore CCR5 binding, suggesting that the CD4 binding site is indeed blocked by JM2.

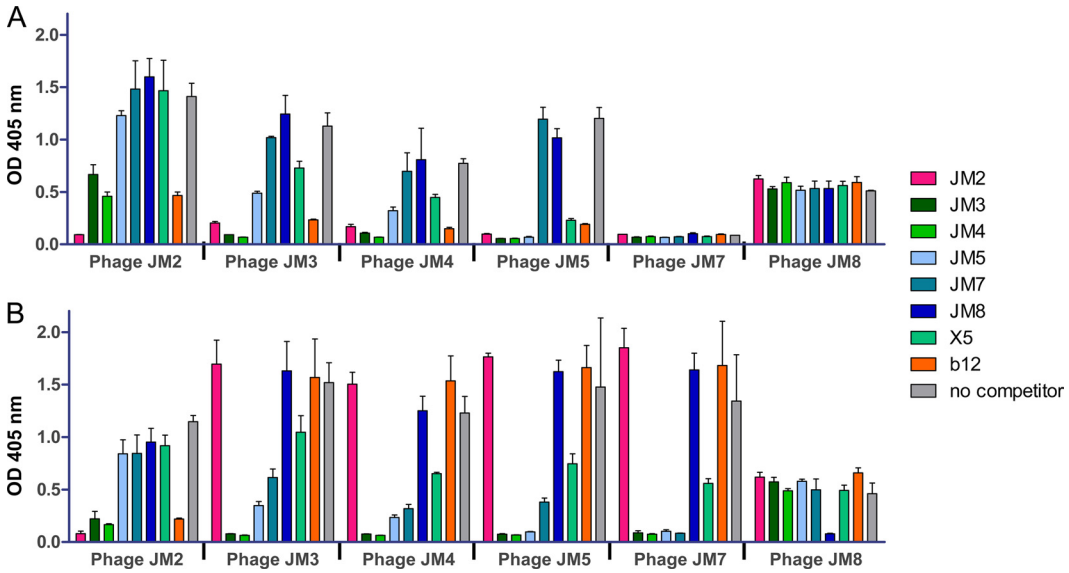

FIG 4 Competition between sdAbs and phage-sdAbs on gp140 or gp140-S-S-M64U1 followed by ELISA. Amounts of 10 μg/ml of sdAbs, X5, and b12 were added to immobilized Env as indicated in Materials and Methods. After 1 h, phage-sdAbs were added at subsaturating concentration. Bound phage-sdAbs were revealed by using peroxidase-labeled anti-M13 antibody. (A) Competition was done on free gp140. (B) Competition was done on gp140-S-S-M64U1. Data from one experiment representative of three independent experiments are shown. Error bars represent standard deviations of the means of triplicates.

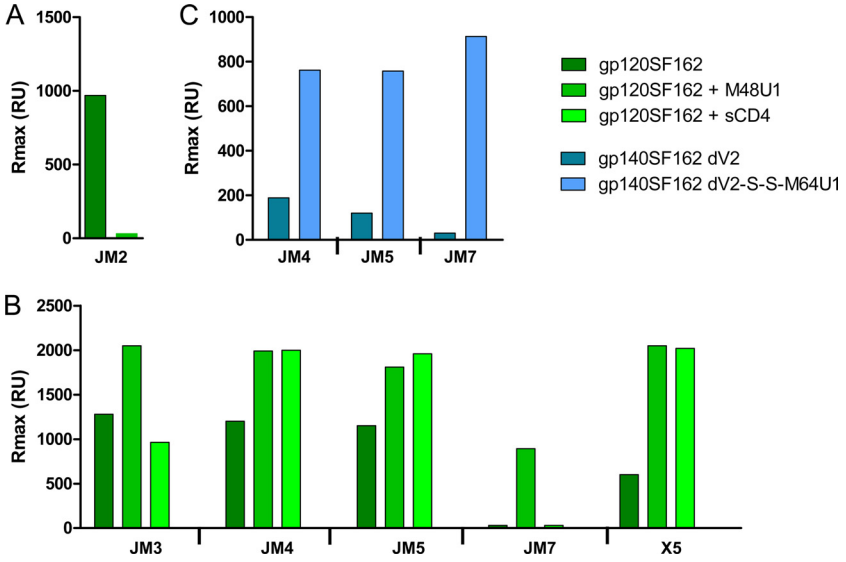

FIG 5 sdAb binding to complexed or uncomplexed Env followed by SPR. sdAbs were immobilized on sensor chip CM5. Using a Biacore 3000 instrument, Env was injected at various concentrations on different channels. Uncomplexed gp120 and gp120-plus-M48U1 complex were run over immobilized JM2 (A) or immobilized JM3, JM4, JM5, and JM7, with MAb X5 as a reference (B). Uncomplexed gp140 and gp140-plus-M48U1 complex were run over immobilized JM4, JM5, and JM7 (C). Data from one experiment representative of three independent experiments are shown. RU, response units.

Characterization of the CD4i sdAbs JM3, JM4, JM5, and JM7. Since our previous ELISA and SPR results suggested that several anti-Env sdAbs, such as JM3, JM4, JM5, and JM7, were targeting the CoRBS unveiled by a conformational change due to CD4 binding (i.e., CD4i epitopes), we used flow cytometry to check whether these sdAbs could block the interaction between gp120-sCD4 or gp120-M48U1 complexes and the CCR5 coreceptor expressed on cells. Figure 7A shows that CD4i sdAbs JM3, JM4, and JM5 could efficiently block the binding of gp120 to CCR5 under all conditions. This experiment also confirmed that JM7 only binds to the Env-M48U1 complex. Indeed, JM7 did not block gp120 or gp120-sCD4 binding to CCR5, but it could bind to gp120 and abolish its binding to the CCR5$^+$ cells in the presence of M48U1. As expected, no gp120 binding was observed by flow cytometry using untransfected CHO cells as negative control (data not shown).

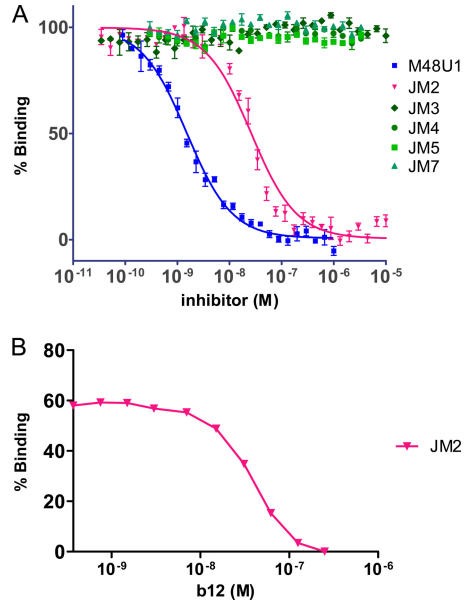

FIG 6 Characterization of CD4BS sdAb. (A) Curves obtained by fluorescence polarization using a fluorescent miniCD4, M64-Fluo, as probe in the presence of various concentrations of sdAbs and miniCD4 M48U1. (B) Competition experiment performed by SPR using various concentrations of MAb b12 mixed with gp120 and injected onto a chip coated with sdAb JM2. Binding of Env on sdAbs is expressed as the percentage of binding compared to that of the control (absence of competitor). Data from one experiment representative of three independent experiments are shown.

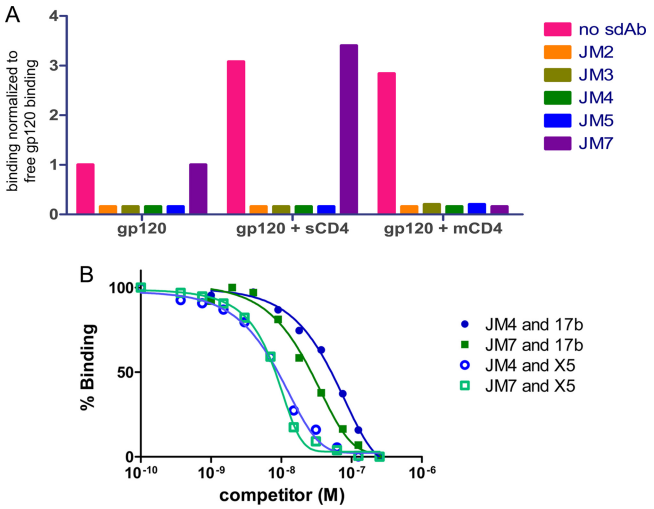

FIG 7 Characterization of CD4i sdAbs. (A) Binding of gp120, gp120-sCD4 complex, and gp120-M48U1 (mCD4) complex to CCR5-expressing cells in the presence of various sdAbs was followed by flow cytometry. gp120 binding to CCR5 was detected by using D7324 anti-gp120 MAb and a secondary antibody labeled with a phycoerythrin moiety. All results are normalized to the binding of free gp120 in the absence of sdAb. (B) Results of SPR competition experiments. gp120-plus-M48U1 complex was run over immobilized sdAbs JM4 and JM7 in the presence of various concentrations of CD4i MAbs 17b and X5. Results are expressed as the percentage of binding obtained in the absence of competing MAb.

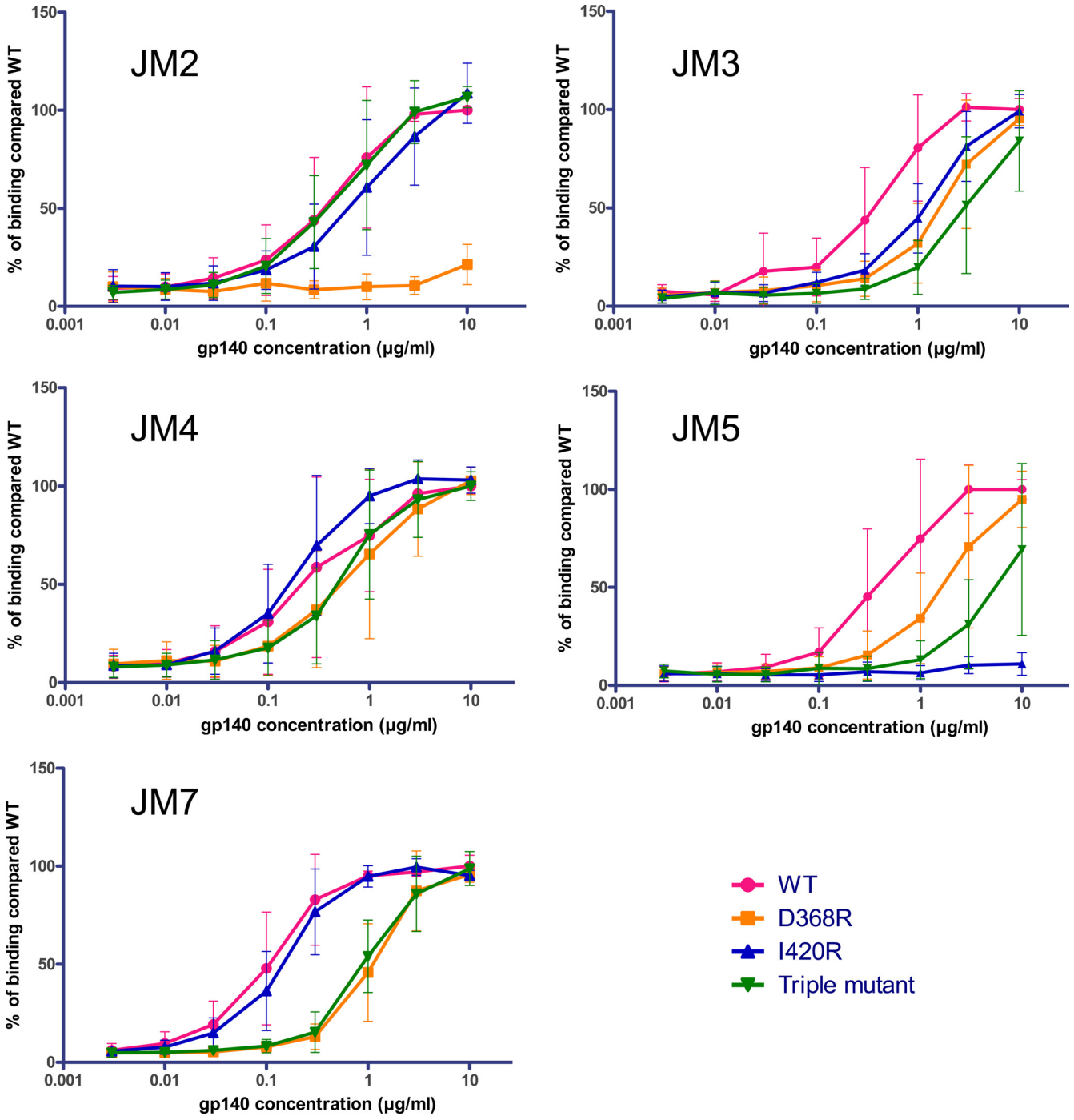

FIG 8 sdAb epitope mapping using Env mutants in ELISA. Each sdAb was assessed for its ability to bind wild-type Env, CD4BS D368R mutant, CoRBS I420R mutant, and triple I423M N425K G431E mutant, all except JM2 in the presence of miniCD4 M48U1. Results are expressed as percentage of binding compared to that of wild-type gp140.

Additional SPR experiments could demonstrate that JM4 and JM7 competed efficiently with the well-characterized CD4i MAbs X5 and 17b (35, 36) for binding to CD4i epitopes (Fig. 7B). Altogether, these results clearly confirm that JM3, JM4, JM5, and JM7 recognize conformational epitopes shared with MAbs X5 and 17b and involved in the interaction of gp120 with the HIV-1 CCR5 coreceptor.

Epitope mapping by ELISA using mutant Env proteins. Well-known Env mutants were used to confirm our previous results. ELISAs were performed using (i) gp140YU2 D368R, which affects the binding of most CD4BS antibodies, (ii) gp140YU2 I420R, which affects the binding of most CoRBS antibodies, and (iii) gp140YU2 I423M N425K G431E, a triple mutant which exhibits both reduced sCD4 and antibody 17b binding (Fig. 8) (34, 37). In

TABLE 3 Affinities of JM2, JM4, and JM7 on uncomplexed or complexed gp120 determined by SPR

sdAb	Uncomplexed gp120			Complexed gp120+M48U1		
	k_a (M^{-1} s^{-1})	k_d (s^{-1})	K_D (M)	k_a (M^{-1} s^{-1})	k_d (s^{-1})	K_D (M)
JM2	1.4×10^4	6.0×10^{-4}	4.3×10^{-8}		NB[a]	
JM4	3.0×10^4	8.9×10^{-5}	2.9×10^{-9}	1.2×10^5	3.9×10^{-6}	3.2×10^{-11}
JM7		NB		4.3×10^5	2.7×10^{-4}	6.4×10^{-10}

[a] NB, no binding.

this assay, JM2 could bind to the I420R and I423M N425K G431E gp140YU2 mutants but not to the D368R mutant, fully confirming its CD4BS binding pattern. JM3 and JM5 presented a lesser ability to bind to the Env mutants than to wild-type Env, but JM5 did not bind to the I420R mutant, confirming its CoRBS binding pattern. JM7 bound equally well to wild-type and I420R mutated Env but showed a decreased affinity for the D368R mutant and the triple mutant, confirming the original binding pattern of JM7. Surprisingly, JM4 binding was not significantly affected by any of the mutations. One explanation may be that JM4 binds to an epitope located near the CoRBS but differing from those recognized by 17b and other CoRBS antibodies.

Affinities of sdAbs JM2, JM4, and JM7 for gp120 determined by surface plasmon resonance. The affinity of representative CD4BS (JM2) and CD4i (JM4) sdAbs for complexed or uncomplexed gp120, as well as the affinity of sdAb JM7 for the gp120/miniCD4 complex, were determined by SPR (Table 3). As expected, no specific binding of JM2 to the complexed gp120 was detected, but the affinity of JM2 for the uncomplexed gp120 was measured, yielding a k_a (association rate) of 1.4×10^4 M^{-1} s^{-1}, a k_d (dissociation rate) of 6.0×10^{-4} s^{-1}, and a calculated K_D (equilibrium dissociation constant) of 43 nM. In contrast, JM7 did not bind to uncomplexed gp120 but yielded a K_D of 0.6 nM for the g120/miniCD4 complex. While the affinity of JM4 measured for the uncomplexed gp120 resulted in a calculated K_D of 3 nM, this sdAb yielded an extremely high affinity for gp120 complexed to the M48U1 CD4 mimic, and the calculated K_D of 32 pM is probably not accurate, since the BIAcore device is not suitable to measure extremely low dissociation rates in the 10^{-6} s^{-1} range.

Neutralizing activities of multivalent sdAb proteins. Finally, we investigated the possibility of increasing the spectrum of neutralization and inhibitory activity (IC_{50}) of our neutralizing sdAbs through the design of several homo- and heteromultivalent constructs using flexible glycine/serine linkers between monovalent sdAbs. Seven homo- or heterobivalent constructs, listed in Table 1, and a single JM4 homotrivalent sdAb (JM4x4x4) were built (see Fig. S1 in the supplemental material), produced, and tested as described previously in a single-round infection assay for their ability to neutralize a significant panel of pseudotyped virions carrying various HIV-1 envelope glycoproteins. The neutralization efficiencies of these molecules were compared to those of the monovalent parental sdAb molecules. Importantly, whereas none of the parental monovalent sdAbs was able to neutralize all pseudovirus particles (Table 1), 3 bivalent proteins (JM2x2, JM3x3, and JM5x3) and the homotrivalent protein (JM4x4x4) were able to at least partly neutralize all tested pseudovirus particles carrying envelopes from different HIV-1 subtypes. For example, virions displaying 92UG037.8 (subtype A) or 93TH976.17 (subtype CRF01_AE) envelopes, which were neutralized by none of the monovalent sdAbs, were efficiently neutralized by the four best multivalent proteins (JM2x2, JM3x3, JM5x3, and JM4x4x4). However, the IC_{50}s of these multivalent constructs were in the range of those measured with monovalent proteins. These results indicate that multimerization of monovalent neutralizing sdAbs resulted here in a much broader spectrum of neutralization but did not modify the relative affinities of these sdAbs.

DISCUSSION

In the present study, we have designed original immunogens to immunize llamas and select single-domain antibodies (sdAbs) targeting various epitopes of HIV-1 Env. Using trimeric soluble forms of the gp140 envelope glycoprotein for immunization and gp120 for selection, we were able to isolate a panel of sdAbs that bound to neutralization-sensitive sites of gp120. While sdAb JM2 recognizes an epitope corresponding to the CD4 binding site (CD4BS) of gp120, sdAbs JM3, JM4, and JM5 bind to epitopes unveiled by the conformational change induced by CD4 binding to gp120 and correspond to CD4-induced (CD4i) antibodies. Since we used the subtype B envelope from the HIV-1 SF162 strain for immunization and selection, these sdAbs exhibited neutralizing activity against viruses expressing subtype B envelopes, including primary viral isolates (tier 2 and tier 2/3) that were resistant to almost all of the broadly neutralizing human monoclonal antibodies that we tested (2G12, b12, 2F5, 4E10, PG9, and PG16). However, sdAb JM3, which presents the broadest neutralization properties, can also neutralize some viruses pseudotyped with A, G, or CRF01_AE envelopes. In addition, the best sdAb candidates, when expressed as multimers, are also efficient in neutralizing a broad panel of viruses carrying envelopes from HIV-1 subtypes A, C, G, and CRF01_AE. Strikingly, two of them, JM3x3 and JM5x3, were able to neutralize all virus subtypes tested.

Using a nonspecific elution to recover the phage bound to the selection antigen, most of the best sdAb candidates isolated were dominant clones from the output of basic phage display-based *in vitro* selection. Interestingly, a large amount of this output was composed of phage-sdAbs specifically binding to relevant epitopes. Indeed, these phage-sdAbs included CD4BS binders but also phage-sdAbs that bound preferentially to the gp120/CD4 mimic complex, therefore targeting CD4-induced epitopes overlapping the CoRBS. Most of the selected binders were directed against epitopes involved in the interaction with a partner (CD4, and CXCR4 or CCR5). This finding is in good agreement with the literature demonstrating the tendency of sdAbs to bind cavities and cryptic epitopes (38). Using different strategies for both immunization and subsequent selection, Forsman and collaborators were able to isolate CD4BS-neutralizing sdAbs (13), but to our knowledge, this is the first time that single-domain antibodies targeting HIV-1 coreceptor binding sites are being described.

Surprisingly, all blocking sdAbs were isolated from selection performed on monomeric gp120, while the immunization had

been performed using trimeric Env (gp140). When selections were performed on gp140, sdAbs that bound specifically to the trimeric conformation and showing no binding activity toward the monomeric gp120 were preferentially selected (sdAbs JM8 and JM9). However, these clones could not efficiently block the infection process in the neutralization assay. It might be that selections on trimeric Env more closely mimic the natural immunization process on entire virus and mainly lead to nonneutralizing gp120 binders, as can be seen in patients, due to the many tricks that HIV-1 has evolved to escape from humoral response.

sdAb JM2 clearly competes with CD4 mimics or MAb b12 for recognition of the CD4 binding site on gp120 or gp140, and its binding, logically, is abolished by the D368R mutation. With an average affinity of 40 nM, it could efficiently block infection of a variety of virus subtypes. JM2 also hampered the binding of CD4i phage-JM3, -JM4, and -JM5 (Fig. 4A). Reciprocally, JM2 displayed on phage is partially hindered by the binding of JM3 and JM4 and, to a lesser extent, JM5. These results suggest that CD4-induced epitopes recognized by JM3, JM4, and JM5 might be located closer to the CD4BS than conventional CD4i epitopes, thereby leading to steric hindrances between CD4BS binders and CoRBS sdAbs, as has already been described (39). However, CD4i MAbs 17b and X5 are still competing with JM3, JM4, and JM5, implying the recognition of proximate epitopes. JM2 might also stabilize a gp120 conformation that is not well recognized by CoRBS sdAbs JM3, JM4, and JM5, as can be observed by flow cytometry for the binding of gp120 to CCR5 in the presence of JM2. Of note, an earlier study showed significant differences in the structure of CD4-gp120 core complex compared to that of b12-gp120 stabilized core complex (9). Interestingly, the main differences occurred on the bridging sheet, precisely in the CD4i binding area. Thus, JM2 seems to stabilize such an alternative gp120 conformation. Nevertheless, a definitive answer will only be obtained by crystal structure studies.

JM7 is intriguing since this sdAb is able to bind with subnanomolar affinity to the gp120/miniCD4 complex but binds neither to gp120 nor to the gp120/sCD4 complex or the CD4 mimic alone. This could be explained through binding to a bimolecular epitope created by the association of miniCD4 and gp120, as observed earlier with MAb 21c, which shares its epitope between gp120 and CD4 (40). An alternative explanation might be that JM7 and sCD4 cannot bind simultaneously to gp120 due to steric hindrance. However, we could demonstrate a competition between JM7 and JM3, JM4, and JM5, as well as CD4i MAb X5, suggesting that these antibodies still at least partly share their epitopes.

The availability of several sdAbs directed against various neutralizing epitopes of gp120 opens the possibility of creating multivalent sdAbs. Hultberg and collaborators have recently demonstrated the possibility of significantly increasing (up to 4,000-fold) the neutralization potency of sdAbs directed against the trimeric Env proteins of several viruses (H5N1 influenza virus, rabies virus, and Rous sarcoma virus) by designing bivalent and trivalent constructs of neutralizing sdAbs (22). This is probably explained by an avidity effect, multivalent sdAbs being able to bind several protomers of the single trimeric Env. They also demonstrated the potential of creating biparatopic constructs by linking two sdAbs targeting different epitopes, yielding molecules with IC_{50}s in the picomolar range and displaying an increased cross-subtype neutralization activity. We therefore used the same approach to generate homo- and heteromultivalent constructs. Unfortunately, no significant improvement of the neutralizing potency of these multivalent proteins in terms of IC_{50}s was observed compared to those of the parental monovalent sdAbs. However, several multivalent sdAbs could neutralize a broader spectrum of pseudotyped virus particles. While no monovalent sdAb could neutralize the whole batch of pseudovirions tested, four multivalent proteins were able to neutralize pseudovirions carrying envelopes from HIV-1 subtypes A, B, C, G, and CRF01_AE. The JM2x2 homobivalent sdAb showed a better activity than the monovalent JM2 sdAb, probably due to an avidity effect. Interestingly, the JM4x4x4 homotrivalent sdAb neutralized a broader spectrum of pseudovirions than JM4 but with equivalent or higher IC_{50}s. Impressively, JM3x3 was able to neutralize all pseudovirions tested. The position of the flexible linker and the conformation of the resulting molecules also seem to be of importance. Indeed, JM5x2 greatly outperformed JM2x5, and a similar difference was observed between JM5x3 and JM3x5. These differences might also be explained by the angle of binding of some of these sdAbs that might be more or less tolerant to the presence of a linker at their N terminus, located near the antigen binding site.

In conclusion, using an original immunogen and phage-display protocol, we have been able to select a panel of single-domain antibodies targeting the binding sites of CD4 and coreceptors on gp120. These sdAbs are capable of neutralizing a broad spectrum of HIV-1 subtypes, including tier 3 primary isolates. Since these antibody fragments are extremely stable and are easy to produce and purify at high levels, they could have a great potential in developing effective prevention strategies against HIV-1 transmission, such as in the development of potent microbicides (41).

ACKNOWLEDGMENTS

The following reagents were obtained through the AIDS Research and Reference Reagent Program, Division of AIDS, NIAID, NIH: pSVIII-92BR025.9, pSVIII-92RW020.5, pSVIII-92UG975.10, and pSVIII-93BR019.4 from Feng Gao and Beatrice Hahn and pSVIII-91US005.11, pSVIII-92HT593.1, pSVIII-92UG037.8, pSVIII-93TH976.17, and pSVIII-93TH966.8 from Beatrice Hahn. We acknowledge D. P. Burton, P. Parren, D. Katinger, I. Srivastava, P. Kwong, and the National Institute for Biological Standards and Control Centre for AIDS Reagents (supported by the European Union Programme EVA contract QLKZ-CT-1999-00609) and the United Kingdom Medical Research Council for the various antibodies (b12, 17b, and X5) and Env plasmids. We also thank M. Parmentier (University of Brussels, Belgium) for the CHO-K1 $CCR5^+$ cell line and S. Brunet and A. Chaillon for their help in neutralization assays.

This work was supported by Inserm, CNRS, Université Paris-Descartes, and grants from the Agence Nationale de Recherche sur le SIDA (ANRS) (S.B., D.B., and L.M.). J.M. was supported by a fellowship from ANRS.

REFERENCES

1. **Stamatatos L, Morris L, Burton DR, Mascola JR.** 2009. Neutralizing antibodies generated during natural HIV-1 infection: good news for an HIV-1 vaccine? Nat. Med. **15**:866–870.
2. **Walker BD, Burton DR.** 2008. Toward an AIDS vaccine. Science **320**:760–764.
3. **Wyatt R, Kwong PD, Desjardins E, Sweet RW, Robinson J, Hendrickson WA, Sodroski JG.** 1998. The antigenic structure of the HIV gp120 envelope glycoprotein. Nature **393**:705–711.
4. **Liu J, Bartesaghi A, Borgnia MJ, Sapiro G, Subramaniam S.** 2008. Molecular architecture of native HIV-1 gp120 trimers. Nature **455**:109–113.
5. **Chen L, Kwon YD, Zhou T, Wu X, O'Dell S, Cavacini L, Hessell AJ, Pancera M, Tang M, Xu L, Yang ZY, Zhang MY, Arthos J, Burton DR, Dimitrov DS, Nabel GJ, Posner MR, Sodroski J, Wyatt R, Mascola JR,**

Kwong PD. 2009. Structural basis of immune evasion at the site of CD4 attachment on HIV-1 gp120. Science **326**:1123–1127.
6. **Gonzalez N, Alvarez A, Alcami J.** 2010. Broadly neutralizing antibodies and their significance for HIV-1 vaccines. Curr. HIV Res. **8**:602–612.
7. **Walker LM, Phogat SK, Chan-Hui PY, Wagner D, Phung P, Goss JL, Wrin T, Simek MD, Fling S, Mitcham JL, Lehrman JK, Priddy FH, Olsen OA, Frey SM, Hammond PW, Kaminsky S, Zamb T, Moyle M, Koff WC, Poignard P, Burton DR.** 2009. Broad and potent neutralizing antibodies from an African donor reveal a new HIV-1 vaccine target. Science **326**:285–289.
8. **Zhou T, Georgiev I, Wu X, Yang ZY, Dai K, Finzi A, Kwon YD, Scheid JF, Shi W, Xu L, Yang Y, Zhu J, Nussenzweig MC, Sodroski J, Shapiro L, Nabel GJ, Mascola JR, Kwong PD.** 2010. Structural basis for broad and potent neutralization of HIV-1 by antibody VRC01. Science **329**:811–817.
9. **Zhou T, Xu L, Dey B, Hessell AJ, Van Ryk D, Xiang SH, Yang X, Zhang MY, Zwick MB, Arthos J, Burton DR, Dimitrov DS, Sodroski J, Wyatt R, Nabel GJ, Kwong PD.** 2007. Structural definition of a conserved neutralization epitope on HIV-1 gp120. Nature **445**:732–737.
10. **Labrijn AF, Poignard P, Raja A, Zwick MB, Delgado K, Franti M, Binley J, Vivona V, Grundner C, Huang CC, Venturi M, Petropoulos CJ, Wrin T, Dimitrov DS, Robinson J, Kwong PD, Wyatt RT, Sodroski J, Burton DR.** 2003. Access of antibody molecules to the conserved coreceptor binding site on glycoprotein gp120 is sterically restricted on primary human immunodeficiency virus type 1. J. Virol. **77**:10557–10565.
11. **Moulard M, Phogat SK, Shu Y, Labrijn AF, Xiao X, Binley JM, Zhang MY, Sidorov IA, Broder CC, Robinson J, Parren PW, Burton DR, Dimitrov DS.** 2002. Broadly cross-reactive HIV-1-neutralizing human monoclonal Fab selected for binding to gp120-CD4-CCR5 complexes. Proc. Natl. Acad. Sci. U. S. A. **99**:6913–6918.
12. **Van Bockstaele F, Holz JB, Revets H.** 2009. The development of nanobodies for therapeutic applications. Curr. Opin. Investig. Drugs **10**:1212–1224.
13. **Forsman A, Beirnaert E, Aasa-Chapman MM, Hoorelbeke B, Hijazi K, Koh W, Tack V, Szynol A, Kelly C, McKnight A, Verrips T, de Haard H, Weiss RA.** 2008. Llama antibody fragments with cross-subtype HIV-1 neutralizing properties and high affinity for HIV-1 gp120. J. Virol. **82**:12069–12081.
14. **Koh WW, Steffensen S, Gonzalez M, Hoorelbeke B, Gorlani A, Szynol A, Forsman A, Aasa-Chapman MM, de Haard H, Verrips T, Weiss RA.** 2010. Generation of a family-specific phage library of llama single chain antibody fragments that neutralize HIV-1. J. Biol. Chem. **285**:19116–19124.
15. **Dey AK, Burke B, Sun Y, Sirokman K, Nandi A, Hartog K, Lian Y, Geonnotti AR, Montefiori D, Franti M, Martin G, Carfi A, Kessler P, Martin L, Srivastava IK, Barnett SW.** 2012. Elicitation of neutralizing antibodies directed against CD4-induced epitope(s) using a CD4 mimetic cross-linked to a HIV-1 envelope glycoprotein. PLoS One **7**:e30233. doi:10.1371/journal.pone.0030233.
16. **Martin G, Burke B, Thai R, Dey AK, Combes O, Ramos OH, Heyd B, Geonnotti AR, Montefiori DC, Kan E, Lian Y, Sun Y, Abache T, Ulmer JB, Madaoui H, Guerois R, Barnett SW, Srivastava IK, Kessler P, Martin L.** 2011. Stabilization of HIV-1 envelope in the CD4-bound conformation through specific cross-linking of a CD4 mimetic. J. Biol. Chem. **286**:21706–21716.
17. **Martin G, Sun Y, Heyd B, Combes O, Ulmer JB, Descours A, Barnett SW, Srivastava IK, Martin L.** 2008. A simple one-step method for the preparation of HIV-1 envelope glycoprotein immunogens based on a CD4 mimic peptide. Virology **381**:241–250.
18. **Martin L, Stricher F, Misse D, Sironi F, Pugniere M, Barthe P, Prado-Gotor R, Freulon I, Magne X, Roumestand C, Menez A, Lusso P, Veas F, Vita C.** 2003. Rational design of a CD4 mimic that inhibits HIV-1 entry and exposes cryptic neutralization epitopes. Nat. Biotechnol. **21**:71–76.
19. **Moscoso CG, Sun Y, Poon S, Xing L, Kan E, Martin L, Green D, Lin F, Vahlne AG, Barnett S, Srivastava I, Cheng RH.** 2011. Quaternary structures of HIV Env immunogen exhibit conformational vicissitudes and interface diminution elicited by ligand binding. Proc. Natl. Acad. Sci. U. S. A. **108**:6091–6096.
20. **Behar G, Chames P, Teulon I, Cornillon A, Alshoukr F, Roquet F, Pugniere M, Teillaud JL, Gruaz-Guyon A, Pelegrin A, Baty D.** 2009. Llama single-domain antibodies directed against nonconventional epitopes of tumor-associated carcinoembryonic antigen absent from nonspecific cross-reacting antigen. FEBS J. **276**:3881–3893.
21. **Van Herrewege Y, Morellato L, Descours A, Aerts L, Michiels J, Heyndrickx L, Martin L, Vanham G.** 2008. CD4 mimetic miniproteins: potent anti-HIV compounds with promising activity as microbicides. J. Antimicrob. Chemother. **61**:818–826.
22. **Hultberg A, Temperton NJ, Rosseels V, Koenders M, Gonzalez-Pajuelo M, Schepens B, Ibanez LI, Vanlandschoot P, Schillemans J, Saunders M, Weiss RA, Saelens X, Melero JA, Verrips CT, Van Gucht S, de Haard HJ.** 2011. Llama-derived single domain antibodies to build multivalent, superpotent and broadened neutralizing anti-viral molecules. PLoS One **6**:e17665. doi:10.1371/journal.pone.0017665.
23. **Studier FW.** 2005. Protein production by auto-induction in high density shaking cultures. Protein Expr. Purif. **41**:207–234.
24. **Wei X, Decker JM, Wang S, Hui H, Kappes JC, Wu X, Salazar-Gonzalez JF, Salazar MG, Kilby JM, Saag MS, Komarova NL, Nowak MA, Hahn BH, Kwong PD, Shaw GM.** 2003. Antibody neutralization and escape by HIV-1. Nature **422**:307–312.
25. **Naldini L, Blomer U, Gallay P, Ory D, Mulligan R, Gage FH, Verma IM, Trono D.** 1996. In vivo gene delivery and stable transduction of nondividing cells by a lentiviral vector. Science **272**:263–267.
26. **Hofmann W, Schubert D, LaBonte J, Munson L, Gibson S, Scammell J, Ferrigno P, Sodroski J.** 1999. Species-specific, postentry barriers to primate immunodeficiency virus infection. J. Virol. **73**:10020–10028.
27. **Laguette N, Benichou S, Basmaciogullari S.** 2009. Human immunodeficiency virus type 1 Nef incorporation into virions does not increase infectivity. J. Virol. **83**:1093–1104.
28. **Barin F, Brunet S, Brand D, Moog C, Peyre R, Damond F, Charneau P, Barre-Sinoussi F.** 2004. Interclade neutralization and enhancement of human immunodeficiency virus type 1 identified by an assay using HeLa cells expressing both CD4 receptor and CXCR4/CCR5 coreceptors. J. Infect. Dis. **189**:322–327.
29. **Chaillon A, Wack T, Braibant M, Mandelbrot L, Blanche S, Warszawski J, Barin F.** 2012. The breadth and titer of maternal HIV-1-specific heterologous neutralizing antibodies are not associated with a lower rate of mother-to-child transmission of HIV-1. J. Virol. **86**:10540–10546.
30. **Dreja H, O'Sullivan E, Pade C, Greene KM, Gao H, Aubin K, Hand J, Isaksen A, D'Souza C, Leber W, Montefiori D, Seaman MS, Anderson J, Orkin C, McKnight A.** 2010. Neutralization activity in a geographically diverse East London cohort of human immunodeficiency virus type 1-infected patients: clade C infection results in a stronger and broader humoral immune response than clade B infection. J. Gen. Virol. **91**:2794–2803.
31. **Simek MD, Rida W, Priddy FH, Pung P, Carrow E, Laufer DS, Lehrman JK, Boaz M, Tarragona-Fiol T, Miiro G, Birungi J, Pozniak A, McPhee DA, Manigart O, Karita E, Inwoley A, Jaoko W, Dehovitz J, Bekker LG, Pitisuttithum P, Paris R, Walker LM, Poignard P, Wrin T, Fast PE, Burton DR, Koff WC.** 2009. Human immunodeficiency virus type 1 elite neutralizers: individuals with broad and potent neutralizing activity identified by using a high-throughput neutralization assay together with an analytical selection algorithm. J. Virol. **83**:7337–7348.
32. **Stricher F, Martin L, Barthe P, Pogenberg V, Mechulam A, Menez A, Roumestand C, Veas F, Royer C, Vita C.** 2005. A high-throughput fluorescence polarization assay specific to the CD4 binding site of HIV-1 glycoproteins based on a fluorescein-labelled CD4 mimic. Biochem. J. **390**:29–39.
33. **Samson M, Labbe O, Mollereau C, Vassart G, Parmentier M.** 1996. Molecular cloning and functional expression of a new human CC-chemokine receptor gene. Biochemistry **35**:3362–3367.
34. **Feng Y, McKee K, Tran K, O'Dell S, Schmidt SD, Phogat A, Forsell MN, Karlsson Hedestam GB, Mascola JR, Wyatt RT.** 2012. Biochemically defined HIV-1 envelope glycoprotein variant immunogens display differential binding and neutralizing specificities to the CD4-binding site. J. Biol. Chem. **287**:5673–5686.
35. **Huang CC, Tang M, Zhang MY, Majeed S, Montabana E, Stanfield RL, Dimitrov DS, Korber B, Sodroski J, Wilson IA, Wyatt R, Kwong PD.** 2005. Structure of a V3-containing HIV-1 gp120 core. Science **310**:1025–1028.
36. **Kwong PD, Wyatt R, Robinson J, Sweet RW, Sodroski J, Hendrickson WA.** 1998. Structure of an HIV gp120 envelope glycoprotein in complex with the CD4 receptor and a neutralizing human antibody. Nature **393**:648–659.
37. **Shrivastava IH, Wendel K, Lalonde JM.** 2012. Spontaneous rearrangement of the beta20/beta21 strands in simulations of unliganded HIV-1 glycoprotein, gp120. Biochemistry **51**:7783–7793.
38. **De Genst E, Silence K, Decanniere K, Conrath K, Loris R, Kinne J,**

Muyldermans S, Wyns L. 2006. Molecular basis for the preferential cleft recognition by dromedary heavy-chain antibodies. Proc. Natl. Acad. Sci. U. S. A. **103**:4586–4591.
39. **Moore JP, Sodroski J.** 1996. Antibody cross-competition analysis of the human immunodeficiency virus type 1 gp120 exterior envelope glycoprotein. J. Virol. **70**:1863–1872.
40. **Diskin R, Marcovecchio PM, Bjorkman PJ.** 2010. Structure of a clade C HIV-1 gp120 bound to CD4 and CD4-induced antibody reveals anti-CD4 polyreactivity. Nat. Struct. Mol. Biol. **17**:608–613.
41. **Gorlani A, Brouwers J, McConville C, van der Bijl P, Malcolm K, Augustijns P, Quigley AF, Weiss R, De Haard H, Verrips T.** 2012. Llama antibody fragments have good potential for application as HIV type 1 topical microbicides. AIDS Res. Hum. Retroviruses **28**:198–205.